Mapping Heat Stress-Induced Core Histone Post-Translational Modifications in *Acropora cervicornis*.

Cassandra N. Fuller[1], Sabrina Mansoor[2], Santiago J. Guzman[1], Lilian Valadares Tose[1], Serena Hackerott[2,3], Javier Rodriguez-Casariego[2,4], Jose M. Eirin-Lopez[2*], Francisco Fernandez-Lima[1,5*]

[1]*Department of Chemistry and Biochemistry, Florida International University, Miami, FL 33199, USA.*

[2]*Environmental Epigenetics Laboratory, Institute of Environment, Florida International University, Miami, FL 33199, USA.*

[3]*College of Earth, Ocean, and Environment, School of Marine Science and Policy, University of Delaware, Lewes, DE 19958, USA*

[4]*Department of Marine Biology and Ecology, Rosenstiel School, University of Miami, Miami, FL 33124, USA.*

[5]*Biomolecular Sciences Institute, Florida International University, Miami, FL 33199, USA.*

Abstract

Histone post-translational modifications (PTMs) participate in the dynamic regulation of chromatin structure and function, through their chemical nature and specific location within the histone sequence. Alternative analytical approaches for histone PTM studies are required to facilitate the differentiation between ubiquitously present isomers and the detection of low-abundance PTMs. Here, we report a high-sensitivity bottom-up method based on nano-liquid chromatography (nLC), trapped ion mobility spectrometry (TIMS), data-dependent acquisition (DDA), parallel accumulation-serial fragmentation (PASEF), and high-resolution time-of-flight tandem mass spectrometry (ToF-MS/MS) for the analysis of histone PTMs. This method was tested in a threatened coral species, the staghorn coral *Acropora cervicornis*, during an episode of acute thermal stress. The obtained results allowed for the identification of PTM changes in core histones involved in the coral's heat response. Compared to traditional LC-MS/MS approaches, the incorporation of TIMS and ddaPASEF MS/MS, resulted in a highly specific and sensitive method with a wide dynamic range (6 orders of magnitude). This depth of analysis allows for the simultaneous measurement of low-abundance PTM signatures relative to the unmodified form. An added advantage is the ability to mass- and mobility-isolate prior to peptide sequencing, resulting in higher confidence identification of epigenetic markers associated with heat stress in corals (e.g., increased H4 4-17 with 2ac and 3ac, and decreases in H4 4-17 K12ac, K16ac, H4 K20me$_2$, and H2A K5ac, K7ac, K9ac, K12ac, K14ac, and K74ac).

Introduction

Histones are small basic proteins which, contrary to a long-held belief, display a high level of diversity within the cell nucleus[1], including the ubiquitous coexistence of genetic variants and multiple proteoforms that bind to DNA and form the fundamental subunit of chromatin known as a nucleosome[2-5]. Within the nucleosome, dimers of the four core histones (H2A, H2B, H3, and H4) bind together to create the octameric face, from which the N- and C-terminal tails protrude[2-4,6-8]. Due to this increased exposure, the highly basic N-terminal tails are especially amenable to interactions with the cellular machinery responsible for post-translational modifications (PTMs). These PTMs (e.g., acetylation [ac], methylation [me_{1-3}], ubiquitination [ub], phosphorylation [ph]) facilitate the modulation in the function of diverse genomic regions in response to abiotic or other biological signals[6,9-11].

Traditionally monitored by antibody-labeling[12-14], alternative analytical methods are required to account for the specificity needed to distinguish between isomeric histone proteoforms, particularly in the case of samples that antibodies remain unavailable for. Mass spectrometry (MS)-based proteomics methods are emerging and continuously evolving in terms of mass accuracy and resolution which can provide a more comprehensive and cost-effective overview of the histone code[15]. Top-down MS proteomics provides annotation on intact proteins using ultrahigh-resolution MS to combat inherent chemical complexity and the biological diversity of histones[16-27]. We have demonstrated the advantages of dual gas-phase separation and complementary fragmentation techniques (e.g., top "double down" MS), which aids in isomeric proteoform separation[20]. Another option is middle-down proteomics, which utilizes enzymes (e.g., chymotrypsin Glu-C, Asp-N) to cleave proteins into large peptides (>3 kDa)[28]. These methods, however, do not reliably account for the high isomeric content of histones due to cleavage being at the tail level (~50 amino acids [AAs]), where a large majority of PTMs occur. To address this, gas-phase pre-separation in combination with electron- or UV-based fragmentation can be employed for adequate peptide sequencing and PTM local elucidation[28-33].

The most common approach to MS proteomics is bottom-up. This method employs proteases (e.g., trypsin, Arg-C[34-36]) that cleave at high-frequency AAs (e.g., lysine and/or arginine in histones) and result in many small peptides (<3 kDa). Trypsin is commonly used due to its robustness and higher efficiency, however, since trypsin cleaves at both lysine and arginine residues, this digestion typically produces many peptides that are too short to yield confident sequence assignment in core histone analysis. To account for this, we have previously published both irreversible (e.g., propionylation) and reversible (e.g., citraconylation) derivatization methods that block lysine residues as cleavage sites[7,37-41]. This facilitates the use of trypsin, which is more cost-effective and robust than Arg-C, and provides slightly longer peptides (still <3 kDa) for analysis. At this shorter peptide level, however, there is still a need to address isomeric content among peptides with multiple PTM sites[38,41]. Recently, we sequenced and annotated *Acropora cervicornis* coral histone H4 proteoforms from a pooled sample set using top-down MS

(https://doi.org/10.34703/gzx1-9v95/MM9SHA)[42] however, appropriate methodology for diversity comparison between individual organisms has yet to be shown.

Here, we describe the analytical value of online nano-liquid chromatography (nLC), trapped ion mobility spectrometry (TIMS), data-dependent acquisition (DDA), parallel accumulation-serial fragmentation (PASEF), and high-resolution tandem time-of-flight (ToF-MS/MS) for the analysis of histone PTMs. With the recent reports of *A. cervicornis* (https://doi.org/10.34703/gzx1-9v95/MM9SHA)[42] histone H4, H2A, and H2B variants and sequences, we now applied bottom-up strategies to demonstrate the sensitivity and applicability of this method to heat stress-induced PTM changes.

Results and Discussion

The histone PTM screening using bottom-up nLC-TIMS-ddaPASEF-ToF MS/MS resulted in the detection of characteristic peptides and their identification based on retention time, mobility, and characteristic fragmentation pattern. Inspection of the 2D IMS-MS contour plot (Figure 1A) shows distinct separation of the peptides based on their charge state; peptides were observed in the 1+ to 3+ charge state range, in good agreement with previous results as a consequence of the derivatization step (i.e., propionylation protocol neutralizes most basic AAs[7,38,41]). Inspection of the 2D LC-IMS contour plot shows the separation of most coeluting peptides, demonstrating the advantages of the added mobility separation prior to MS/MS (Figure 1B).

A target list based on H4, H2A, and H2B variants detected in *Acropora cervicornis* coral (H4, H4.S, H2A, H2A.A, H2B-1, H2B-2, H2B-2K, and H2B-3; https://doi.org/10.34703/gzx1-9v95/MM9SHA)[42] was used for the verification of the high-sensitivity nLC-TIMS-ddaPASEF-ToF MS/MS method as applied to the analysis of coral response to heat stress exposure (e.g., control and heat-exposed). Inspection of the LC-TIMS-MS/MS analysis resulted in the observation of 84 molecular targets (out of 346 possible molecular targets) corresponding to 8 H4, 7 H2A, and 12 H2B peptides with varying PTMs (Table S1 and Figures 2-4 and S1-6). Noteworthy is the high reproducibility, sensitivity, and depth of the analysis, which allows the detection of low-abundant peptides and PTMs across six orders of magnitude.

Inspection of the PTM profiles showed correlation with heat exposure across the samples. The number of acetylations on peptide H4 4-17 rose in exposed samples (up to 3ac) versus control samples (up to 1ac). In control samples, the H4 4-17 peptide is only observed in the unmodified and 1ac form (e.g., K8ac 2+ and 3+, K12ac 2+ and 3+, and K16ac 2+ and 3+). However, exposed samples show an increase up to 2 and 3ac, which were below the limit of detection in the control samples (Figures 1C, 2A, and S1-2). In both sample groups, H4 4-17 acetylations were observed at K8ac (2+ and 3+), K12ac (2+ and 3+), and K16ac (2+ and 3+). Of the H4 4-17 1ac peptides, K12ac 3+, and K16ac 2+ and 3+ were found to be reduced in the exposed corals, likely due to the increase of peptides with additional acetylations (2-3ac, Figures 1C, 2A, S1-2, and Table S2). H4

4-17 peptides with 2ac (K5acK8ac 2+, K5acK12ac 2+, K5acK16ac 2+, K8acK12ac 2+, K8acK16ac 2+, and K12acK16ac 2+) or 3ac (K5acK8acK12ac 2+, K5acK8acK16ac 2+, K5acK12acK16ac 2+, and K8acK12acK16ac 2+) were only observed in the exposed coral samples (Figure 2A and S1-2). All 2 and 3ac H4 4-17 peptides were enriched in the exposed coral samples, compared to the control samples (Figures 1C, 2A, S1-2, and Table S2). The H4 20-23 peptide was observed in the unmodified, K20me$_1$, K20me$_2$, and K20ac forms (Figure 2A and S1-2). The H4 20-23 K20me$_2$ 1+ peptide feature was reduced in the exposed coral samples (Figure 1C and Table S2). All other H4 peptide features (H4 24-35, 40-45, 46-55, 68-78, 79-92, 96-102, and H4.S 79-92) were observed in the unmodified form (Figures S1-2).

The H2A 4-16 peptide is observed in both sample groups in the 1ac (K5ac, K7ac, K9ac, K12ac, and K14ac) and 2ac (K5acK7ac, K5acK9ac, K5acK12ac, K7acK9ac, K7acK12ac, K7ac, K14ac, K9acK12ac, K9acK14ac, and K12acK14ac) forms (Figures 3A and S3-4). However, the exposed samples show a decrease of 1ac peptides features (K5ac 3+, K7ac 3+, K9ac 3+, K12ac 3+, and K14ac 2+ and 3+), primarily in the 3+ charge state forms (Figures 1C, 3A, S3-4, and Table S2). Similarly, H2A 71-76 K74ac (1+ and 2+) was reduced in exposed samples compared to control samples (Figure 1C and Table S2). All other H2A peptide features (H2A 20-28, 29-34, 35-41, 42-70, and 81-87) were observed in the unmodified form (Figures 3A and S3-4). The H2B (2,2K,3) 1-12 peptide was observed in the unmodified, N-me$_2$A, and N-me$_3$A forms in both sample groups (Figures 4A and S5-6). In the exposed samples, an increase of H2B (2,2K,3) 1-12 N-me$_3$A 2+ and 3+ peptide features were observed compared to the control group (Figures 1C , 4A, S5-6, and Table S2). All other H2B peptide features [H2B (2) 13-26, (2K) 13-27, (3) 13-26, (1,2) 26-30, (1,2,2K) 27-30, (3) 26-30, (1) 70-76, (2,2K,3) 70-76, 77-89, 90-96, 97-722] were observed in the unmodified form (Figures 4A and S5-6).

Clustering of the samples by heat exposure treatment indicates a clear distinction between control and exposed sample responses to heat stress for H4 (Figure 2B), H2A (Figure 3B), and H2B (Figure 4B) PTMs. The sample comparison between treatments shows tight clustering among most similar PTMs (e.g., H4 4-17 1ac, 2ac, and 3ac, Figure 2B; H2A 4-16 1ac and 2ac, Figure 3B; H2B (2,2K,3) 1-12 N-me$_2$A and N-me$_3$A, Figure 4B). Additionally, clustering is observed between some peptide features with similar PTMs and charge states (i.e., H4 4-17 K12ac 3+ and K16ac 3+, Figure 2B; H2A 4-16 K5ac 3+ and K7ac 3+, Figure 3B) as well as some peptides detected at multiple charge states (i.e., H4 20-23 K20me$_2$ 1+ and 2+, Figure 2B; H2A K12ac 2+ and 3+, and H2A K14ac 2+ and 3+, Figure 3B). These types of observations are expected, as peptides with multiple charge states observed would see similar decreases/increases within each charge state relevant to total peptide abundance.

Understanding changes in the epigenetic marks in corals is critical to advance our interpretation and propose gene regulation mechanisms and pathways. In particular, the elucidation and quantification of histone PTMs requires advanced analytical detection methods due to the ubiquitously high isomeric content and dynamic range. Online nLC-TIMS-ddaPASEF-ToF

MS/MS can be efficiently used for the bottom-up analysis of derivatized histone peptides when applied to the *Acropora cervicornis* Caribbean staghorn coral.

A high diversity of core histone PTMs was observed in response to heat stress. The inspection of *Acropora cervicornis* H4, H4.S, H2A, H2A.A, H2B-1, H2B-2, H2B-2K, and H2B-3 showed the presence of varying numbers of acetylation (0-3ac) and methylation (me_{0-3}), mostly in the tail positions. The analysis was aided by the ability to isolate mass- and mobility-selected precursors for increased peptide assignment by increasing signal-to-noise and reducing the number of interfering ions[38,41], despite the high diversity of PTMs among samples. When compared, increases in H4 4-17 with 2ac and 3ac, and decreases in H4 4-17 K12ac, K16ac, H4 K20me_2, and H2A K5ac, K7ac, K9ac, K12ac, K14ac, and K74ac were observed from corals exposed to heat stress (exposed) versus those held at ambient temperature (control). While a direct correlation between these PTMs and chromatin remodeling remains to be elucidated, previous reports have shown their involvement in gene transcription[43,44], DNA replication[45], and DNA damage repair[46]. This work introduced a new analytical workflow capable of characterizing chromatin composition in corals, providing the community with tools for future longitudinal studies and the evaluation of responses of other non-model organisms to environmental change.

Materials and Methods

Sample Preparation.

Acropora cervicornis (staghorn) corals were obtained from the Coral Reef Foundation (CRF) nursery located at Tavernier, Florida (N 24.982715°, W -80.436286°) and were propagated under CRF's permit #FKNMS-2019-012-A2. Fragments represented clones of a single coral genotype (CRF AC112) to limit genetic variability during method development. Corals were separated into two temperature treatments including an ambient control (ctrl; n=3) and heat-exposed (exp; n=3) group. Corals in the ambient control treatment group were maintained at 26 °C while heat-exposed corals were subjected to acute (13h) heat stress with a maximum temperature of 33 °C with the aim of inducing a detectable molecular response to thermal stress.

Histones were extracted from collected fragments of each coral treatment group (~10 cm each). Briefly, coral fragments were flash-frozen in liquid nitrogen and ground into a fine powder using a mortar and pestle. The calcium carbonate skeleton was removed from the coral tissue by suspending the powdered coral (~250 mg/mL) in chilled 1X Pre-lysis buffer (EpiQuik™ Total Histone Extraction Kit, EpigenTek, Farmingdale, NY) on ice for 10 min to allow carbonate deposition[43]. The tissue slurry was carefully transferred to a Dounce homogenizer to continue the lysis and histone acid-extraction using the EpiQuik™ Total Histone Extraction Kit. Acid-soluble proteins were subjected to acetone precipitation overnight as previously described[44]. The total protein concentration was determined using the Qubit Protein Assay Kit (Invitrogen:

Carlsbad, CA). Isolated histones were re-suspended in water and stored at -80 °C until ready for further preparation steps.

The extracted histones were derivatized (propionylated, pr), as previously described[7,37,38,40,41,45]. Briefly, histones were solubilized in 100 mM NH_4CO_3 (1 µg/µL, pH 8) and propionylation reagent (1:3 v/v propionic anhydride:acetonitrile[ACN]) was added (1:4 v/v), followed quickly by NH_4OH (1:5 v/v) to maintain a pH of 8. The samples were incubated for 15 min, then this procedure was repeated once before drying *via* vacuum centrifuge. Propionylated histones were reconstituted in NH_4CO_3 (1 µg/µL) and digested using trypsin (1:10 wt/wt)[40] overnight at room temperature. The digest was halted by freezing at -80 °C for at least 1 h, then samples were thawed and dried. The derivatization procedure was repeated as before to propionylate the newly formed peptide N-terminals. Fully propionylated peptide samples were desalted using homemade stage-tips, as previously described[37,38,41]. The C_{18} tips were activated using ACN, followed by equilibration with 0.1% trifluoroacetic acid (TFA). Sample pH was reduced to 4 using glacial acetic acid, then samples were loaded onto the C_{18} material and washed once with 0.1% TFA before elution using 0.5% acetic acid in 75% ACN. Desalted samples were dried, resuspended in 0.1% formic acid (FA), and spiked with custom histone-like QC peptides to monitor the reproducibility of the bottom-up MS method.

Bottom-up Histone PTM screening.

A nanoElute 2 nLC system fitted with a C_{18} column (15 cm x 150 µm i.d., 1.5 µm, Bruker PepSeq column) kept at 50 °C was coupled to a commercial timsTOF Pro2 mass spectrometer (Bruker Daltonics, Billerica, MA). The nLC separation gradient using 0.1% FA in water (mobile phase A) and 0.1% FA in ACN (mobile phase B) started at 2% B and continued as follows: i) 0-60 min to 35% B, ii) 60-69 min to 95% B, iii) 70-78 min to 2% B. Each injection consisted of 1 µL of sample containing 250 ng/µL propionylated coral histone peptides and 25 ng/µL spiked QC peptide (GVKFRGSTGGKAPRGKAPATSGMVGPHR, 2765.54 Da); the QC peptide can be traced using the final QC1 (pr-GSTGGK(pr)APR, 471.75^{2+}) and QC2 (pr-GK(pr)APATSGMVGPHR, 739.38^{2+}) propionylated digest targets. A CaptiveSpray nanoESI source (Bruker Daltonics) operated at 1200 V and flow rate of 500 nL/min was used as the nLC-MS interface. Tandem MS/MS was performed using CID on mobility and *m/z* selected precursor ions in ddaPASEF mode over a range of 0.60-1.80 $1/K_0$ and 100-1700 *m/z* (1+ to 4+ charge states), respectively, while CID collision energy was stepped as a function of both *m/z* and $1/K_0$, as previously described[37,41]. The limit of detection (LOD) is specific to each peptide target and charge state; to evaluate the fold changes, the LOD was estimated as the lowest value observed for a known peptide signal in a biological histone pulldown (see Figure S7).

Histone PTM Data Analysis.

The bottom-up nLC-TIMS-PASEF-ToF MS/MS data was analyzed using a custom script in DataAnalysis software (DA, v6.1, Bruker Daltonics) that considered *m/z*, mobility ($1/K_0$), and retention time from a predetermined list of derivatized histone peptide sequences with varying

PTMs (e.g., ac, me_{1-3}). A target list based on H4, H2A, and H2B variants detected in *Acropora cervicornis* coral (H4, H4.S, H2A, H2A.A, H2B-1, H2B-2, H2B-2K, and H2B-3; https://doi.org/10.34703/gzx1-9v95/MM9SHA)[42] was used. The histone H3 sequence has not been reported and therefore was not included[42]. The QC1 and QC2 peptides were used as a measure of the analytical reproducibility and analysis performance. Mobility and mass method calibration was performed using hexakis(2,2-difluoroethoxy) phosphazine, hexakis(2,2,3,3-tetrafluoropropoxy) phosphazine, and hexakis(1H, 1H, 7H-dodecafluoroheptoxy) phosphazine standards (Apollo Scientific Ltd, UK). The reported peptides and PTMs were manually curated using the isotopic profile of the precursor mass (± 0.01 Da), previously reported peptide mobility profile patterns (including positional isomers, RSD < 2%)[41], and MS/MS fragmentation patterns. Extracted ion mass and mobility filtered chromatograms were extracted using the DA script and normalized to the area of QC peptides (e.g., QC1).

Associated Content

Data Availability Statement

Bottom-up nLC-TIMS-ddaPASEF-ToF MS/MS raw data for all ambient control and heat-exposed *Acropora cervicornis* samples is freely accessible at *via* the FIU Research Data Repository at https://doi.org/10.34703/gzx1-9v95/3MF7D3.

Top-down LC-MS, nESI-ToF and nESI-q-ECD-ToF MS/MS raw data for *Acropora cervicornis* histone H4 variant sequences is freely accessible *via* the FIU Research Data Repository at https://doi.org/10.34703/gzx1-9v95/MM9SHA.

Supporting Information

Supplementary Figures S1-7 and Tables S1-2 are available at *EnvEpig* online.

Acknowledgements

The authors acknowledge the financial support from the National Institutes of General Medicine (R35GM153450) to FFL and the National Science Foundation (1921402) to JEL. CNF acknowledges the fellowship support from the National Science Foundation (HRD-1547798 and HRD-2111661). These NSF grants were awarded to Florida International University as part of the Centers of Research Excellence in Science and Technology (CREST) Program. This is contribution number 1992 from the Institute of Environment, a Preeminent Program at Florida International University.

Author Information

Corresponding Authors

***Francisco Fernandez-Lima** – *Department of Chemistry and Biochemistry, Florida International University, Miami, FL 33199, USA*; *Biomolecular Sciences Institute, Florida International University, Miami, FL 33199*; ORCID 0000-0002-1283-4390; Email: fernandf@fiu.edu

***Jose M. Eirin-Lopez** - *Environmental Epigenetics Laboratory, Institute of Environment, Florida International University, Miami, FL 33199, USA*; ORCID 0000-0002-8041-9770; Email: jeirinlo@fiu.edu

Authors

Cassandra N. Fuller - *Department of Chemistry and Biochemistry, Florida International University, Miami, FL 33199, USA*; https://orcid.org/0009-0004-0412-7639

Sabrina Mansoor – *Environmental Epigenetics Laboratory, Institute of Environment, Florida International University, Miami, FL 33199, USA*; https://orcid.org/0009-0002-4756-4463

Santiago J. Guzman - *Department of Chemistry and Biochemistry, Florida International University, Miami, FL 33199, USA*

Lilian Valadares Tose – *Department of Chemistry and Biochemistry, Florida International University, Miami, FL 33199, USA*; https://orcid.org/0000-0001-7445-7503

Serena Hackerott - *Environmental Epigenetics Laboratory, Institute of Environment, Florida International University, Miami, FL 33199, USA*; *College of Earth, Ocean, and Environment, School of Marine Science and Policy, University of Delaware, Lewes, DE 19958, USA;* https://orcid.org/0000-0001-6462-9885

Javier Rodriguez-Casariego – *Environmental Epigenetics Laboratory, Institute of Environment, Florida International University, Miami, FL 33199, USA*; *Department of Marine Biology and Ecology, Rosenstiel School, University of Miami, Key Biscayne, FL 33149, USA*; https://orcid.org/0000-0001-9955-4721

Author Contributions

FFL, JMEL, and SH conceived and designed the study. SH performed biological experiments. SM and JRC optimized and performed histone extractions. CNF performed histone derivatization and digestion. CNF and LVT performed analytical experiments and acquired the data. CNF and SJG analyzed the data. CNF and FFL wrote the paper. All authors edited and approved the manuscript.

References

1. González-Romero, R., Rivera-Casas, C., Frehlick, L.J., Méndez, J., Ausió, J. and Eirín-López, J.M. (2012) Histone H2A (H2A.X and H2A.Z) Variants in Molluscs: Molecular Characterization and Potential Implications For Chromatin Dynamics. *PLOS ONE*, **7**, e30006.
2. Luger, K., Mäder, A.W., Richmond, R.K., Sargent, D.F. and Richmond, T.J. (1997) Crystal structure of the nucleosome core particle at 2.8 A resolution. *Nature*, **389**, 251-260.
3. Peterson, C.L. and Laniel, M.A. (2004) Histones and histone modifications. *Curr Biol*, **14**, R546-551.
4. Turner, B.M. (2002) Cellular memory and the histone code. *Cell*, **111**, 285-291.
5. Zlatanova, J., Bishop, T.C., Victor, J.M., Jackson, V. and van Holde, K. (2009) The nucleosome family: dynamic and growing. *Structure*, **17**, 160-171.
6. Berger, S.L. (2002) Histone modifications in transcriptional regulation. *Curr Opin Genet Dev*, **12**, 142-148.
7. Garcia, B.A., Mollah, S., Ueberheide, B.M., Busby, S.A., Muratore, T.L., Shabanowitz, J. and Hunt, D.F. (2007) Chemical derivatization of histones for facilitated analysis by mass spectrometry. *Nat Protoc*, **2**, 933-938.
8. Spotswood, H.T. and Turner, B.M. (2002) An increasingly complex code. *J Clin Invest*, **110**, 577-582.
9. Bannister, A.J. and Kouzarides, T. (2011) Regulation of chromatin by histone modifications. *Cell Research*, **21**, 381-395.
10. Jenuwein, T. and Allis, C.D. (2001) Translating the histone code. *Science*, **293**, 1074-1080.
11. Zhou, X., Cain, C.E., Myrthil, M., Lewellen, N., Michelini, K., Davenport, E.R., Stephens, M., Pritchard, J.K. and Gilad, Y. (2014) Epigenetic modifications are associated with inter-species gene expression variation in primates. *Genome Biol*, **15**, 547.
12. Kimura, H., Hayashi-Takanaka, Y., Goto, Y., Takizawa, N. and Nozaki, N. (2008) The organization of histone H3 modifications as revealed by a panel of specific monoclonal antibodies. *Cell Struct Funct*, **33**, 61-73.
13. Turner, B.M., O'Neill, L.P. and Allan, I.M. (1989) Histone H4 acetylation in human cells. Frequency of acetylation at different sites defined by immunolabeling with site-specific antibodies. *FEBS Lett*, **253**, 141-145.
14. Wang, H., Huang, Z.Q., Xia, L., Feng, Q., Erdjument-Bromage, H., Strahl, B.D., Briggs, S.D., Allis, C.D., Wong, J., Tempst, P. *et al.* (2001) Methylation of histone H4 at arginine 3 facilitating transcriptional activation by nuclear hormone receptor. *Science*, **293**, 853-857.
15. Moradian, A., Kalli, A., Sweredoski, M.J. and Hess, S. (2014) The top-down, middle-down, and bottom-up mass spectrometry approaches for characterization of histone variants and their post-translational modifications. *Proteomics*, **14**, 489-497.
16. Anderson, L.C., Karch, K.R., Ugrin, S.A., Coradin, M., English, A.M., Sidoli, S., Shabanowitz, J., Garcia, B.A. and Hunt, D.F. (2016) Analyses of Histone Proteoforms Using Front-end Electron Transfer Dissociation-enabled Orbitrap Instruments*. *Molecular & Cellular Proteomics*, **15**, 975-988.

17. Berthias, F., Bilgin, N., Mecinović, J. and Jensen, O.N. (2024) Top-down ion mobility/mass spectrometry reveals enzyme specificity: Separation and sequencing of isomeric proteoforms. *Proteomics*, **24**, e2200471.
18. Dang, X., Singh, A., Spetman, B.D., Nolan, K.D., Isaacs, J.S., Dennis, J.H., Dalton, S., Marshall, A.G. and Young, N.L. (2016) Label-Free Relative Quantitation of Isobaric and Isomeric Human Histone H2A and H2B Variants by Fourier Transform Ion Cyclotron Resonance Top-Down MS/MS. *J Proteome Res*, **15**, 3196-3203.
19. Donnelly, D.P., Rawlins, C.M., DeHart, C.J., Fornelli, L., Schachner, L.F., Lin, Z., Lippens, J.L., Aluri, K.C., Sarin, R., Chen, B. *et al.* (2019) Best practices and benchmarks for intact protein analysis for top-down mass spectrometry. *Nature Methods*, **16**, 587-594.
20. Jeanne Dit Fouque, K., Miller, S.A., Pham, K., Bhanu, N.V., Cintron-Diaz, Y.L., Leyva, D., Kaplan, D., Voinov, V.G., Ridgeway, M.E., Park, M.A. *et al.* (2022) Top-"Double-Down" Mass Spectrometry of Histone H4 Proteoforms: Tandem Ultraviolet-Photon and Mobility/Mass-Selected Electron Capture Dissociations. *Anal Chem*, **94**, 15377-15385.
21. Li, H., Nguyen, H.H., Ogorzalek Loo, R.R., Campuzano, I.D.G. and Loo, J.A. (2018) An integrated native mass spectrometry and top-down proteomics method that connects sequence to structure and function of macromolecular complexes. *Nature Chemistry*, **10**, 139-148.
22. Roberts, D.S., Loo, J.A., Tsybin, Y.O., Liu, X., Wu, S., Chamot-Rooke, J., Agar, J.N., Paša-Tolić, L., Smith, L.M. and Ge, Y. (2024) Top-down proteomics. *Nature Reviews Methods Primers*, **4**, 38.
23. Schachner, L.F., Jooß, K., Morgan, M.A., Piunti, A., Meiners, M.J., Kafader, J.O., Lee, A.S., Iwanaszko, M., Cheek, M.A., Burg, J.M. *et al.* (2021) Decoding the protein composition of whole nucleosomes with Nuc-MS. *Nat Methods*, **18**, 303-308.
24. Smith, L.M. and Kelleher, N.L. (2013) Proteoform: a single term describing protein complexity. *Nat Methods*, **10**, 186-187.
25. Walker, J.N., Lam, R. and Brodbelt, J.S. (2023) Enhanced Characterization of Histones Using 193 nm Ultraviolet Photodissociation and Proton Transfer Charge Reduction. *Anal Chem*, **95**, 5985-5993.
26. Wang, Q., Fang, F., Wang, Q. and Sun, L. (2024) Capillary zone electrophoresis-high field asymmetric ion mobility spectrometry-tandem mass spectrometry for top-down characterization of histone proteoforms. *Proteomics*, **24**, e2200389.
27. Zhang, H., Cui, W., Wen, J., Blankenship, R.E. and Gross, M.L. (2011) Native electrospray and electron-capture dissociation FTICR mass spectrometry for top-down studies of protein assemblies. *Anal Chem*, **83**, 5598-5606.
28. Jiang, T., Hoover, M.E., Holt, M.V., Freitas, M.A., Marshall, A.G. and Young, N.L. (2018) Middle-Down Characterization of the Cell Cycle Dependence of Histone H4 Posttranslational Modifications and Proteoforms. *Proteomics*, **18**, e1700442.
29. Berthias, F., Cooper-Shepherd, D.A., Holck, F.H.V., Langridge, J.I. and Jensen, O.N. (2023) Full Separation and Sequencing of Isomeric Proteoforms in the Middle-Down Mass Range Using Cyclic Ion Mobility and Electron Capture Dissociation. *Analytical Chemistry*, **95**, 11141-11148.

30. Jeanne Dit Fouque, K., Kaplan, D., Voinov, V.G., Holck, F.H.V., Jensen, O.N. and Fernandez-Lima, F. (2021) Proteoform Differentiation using Tandem Trapped Ion Mobility, Electron Capture Dissociation, and ToF Mass Spectrometry. *Anal Chem*, **93**, 9575-9582.
31. Miller, S.A., Jeanne Dit Fouque, K., Hard, E.R., Balana, A.T., Kaplan, D., Voinov, V.G., Ridgeway, M.E., Park, M.A., Anderson, G.A., Pratt, M.R. *et al.* (2023) Top/Middle-Down Characterization of α-Synuclein Glycoforms. *Anal Chem*, **95**, 18039-18045.
32. Miller, S.A., Jeanne Dit Fouque, K., Ridgeway, M.E., Park, M.A. and Fernandez-Lima, F. (2022) Trapped Ion Mobility Spectrometry, Ultraviolet Photodissociation, and Time-of-Flight Mass Spectrometry for Gas-Phase Peptide Isobars/Isomers/Conformers Discrimination. *J Am Soc Mass Spectrom*, **33**, 1267-1275.
33. Shliaha, P.V., Gorshkov, V., Kovalchuk, S.I., Schwämmle, V., Baird, M.A., Shvartsburg, A.A. and Jensen, O.N. (2020) Middle-Down Proteomic Analyses with Ion Mobility Separations of Endogenous Isomeric Proteoforms. *Anal Chem*, **92**, 2364-2368.
34. McKittrick, E., Gafken, P.R., Ahmad, K. and Henikoff, S. (2004) Histone H3.3 is enriched in covalent modifications associated with active chromatin. *Proc Natl Acad Sci U S A*, **101**, 1525-1530.
35. Zhang, K., Tang, H., Huang, L., Blankenship, J.W., Jones, P.R., Xiang, F., Yau, P.M. and Burlingame, A.L. (2002) Identification of Acetylation and Methylation Sites of Histone H3 from Chicken Erythrocytes by High-Accuracy Matrix-Assisted Laser Desorption Ionization–Time-of-Flight, Matrix-Assisted Laser Desorption Ionization–Postsource Decay, and Nanoelectrospray Ionization Tandem Mass Spectrometry. *Analytical Biochemistry*, **306**, 259-269.
36. Zhang, L., Eugeni, E.E., Parthun, M.R. and Freitas, M.A. (2003) Identification of novel histone post-translational modifications by peptide mass fingerprinting. *Chromosoma*, **112**, 77-86.
37. Fernandez-Rojas, M., Fuller, C.N., Valadares Tose, L., Willetts, M., Park, M.A., Bhanu, N.V., Garcia, B.A. and Fernandez-Lima, F. (2024) Histone Modification Screening using Liquid Chromatography, Trapped Ion Mobility Spectrometry, and Time-Of-Flight Mass Spectrometry. *J Vis Exp*.
38. Fuller, C.N., Jeanne Dit Fouque, K., Valadares Tose, L., Vitorino, F.N.L., Garcia, B.A. and Fernandez-Lima, F. (2024) Online, Bottom-up Characterization of Histone H4 4–17 Isomers. *Analytical Chemistry*, **96**, 17165-17173.
39. Karch, K.R., Sidoli, S. and Garcia, B.A. (2016) Identification and Quantification of Histone PTMs Using High-Resolution Mass Spectrometry. *Methods Enzymol*, **574**, 3-29.
40. Sidoli, S., Bhanu, N.V., Karch, K.R., Wang, X. and Garcia, B.A. (2016) Complete Workflow for Analysis of Histone Post-translational Modifications Using Bottom-up Mass Spectrometry: From Histone Extraction to Data Analysis. *J Vis Exp*.
41. Fuller, C.N., Valadares Tose, L., Vitorino, F.N.L., Bhanu, N.V., Panczyk, E.M., Park, M.A., Garcia, B.A. and Fernandez-Lima, F. (2024) Bottom-up Histone Post-translational Modification Analysis using Liquid Chromatography, Trapped Ion Mobility Spectrometry, and Tandem Mass Spectrometry. *Journal of Proteome Research*, **23**, 3867-3876.
42. Fuller, C.N., Mansoor, S., Jeanne Dit Fouque, K., Valadares Tose, L., Rodriguez-Casariego, J., Kosmopoulou, M., Suckau, D., Vitorino, F.N.L., Garcia, B.A., Eirin-Lopez, J.M. *et al.* (2025)

Direct histone proteoform profiling of the unannotated, endangered coral *Acropora cervicornis*. *In review at Nucleic Acids Res.*

43. Martin, B.J.E., Brind'Amour, J., Kuzmin, A., Jensen, K.N., Liu, Z.C., Lorincz, M. and Howe, L.J. (2021) Transcription shapes genome-wide histone acetylation patterns. *Nat Commun*, **12**, 210.
44. Vettese-Dadey, M., Grant, P.A., Hebbes, T.R., Crane- Robinson, C., Allis, C.D. and Workman, J.L. (1996) Acetylation of histone H4 plays a primary role in enhancing transcription factor binding to nucleosomal DNA in vitro. *Embo j*, **15**, 2508-2518.
45. Ruan, K., Yamamoto, T.G., Asakawa, H., Chikashige, Y., Kimura, H., Masukata, H., Haraguchi, T. and Hiraoka, Y. (2015) Histone H4 acetylation required for chromatin decompaction during DNA replication. *Sci Rep*, **5**, 12720.
46. Dhar, S., Gursoy-Yuzugullu, O., Parasuram, R. and Price, B.D. (2017) The tale of a tail: histone H4 acetylation and the repair of DNA breaks. *Philos Trans R Soc Lond B Biol Sci*, **372**.

Figure 1

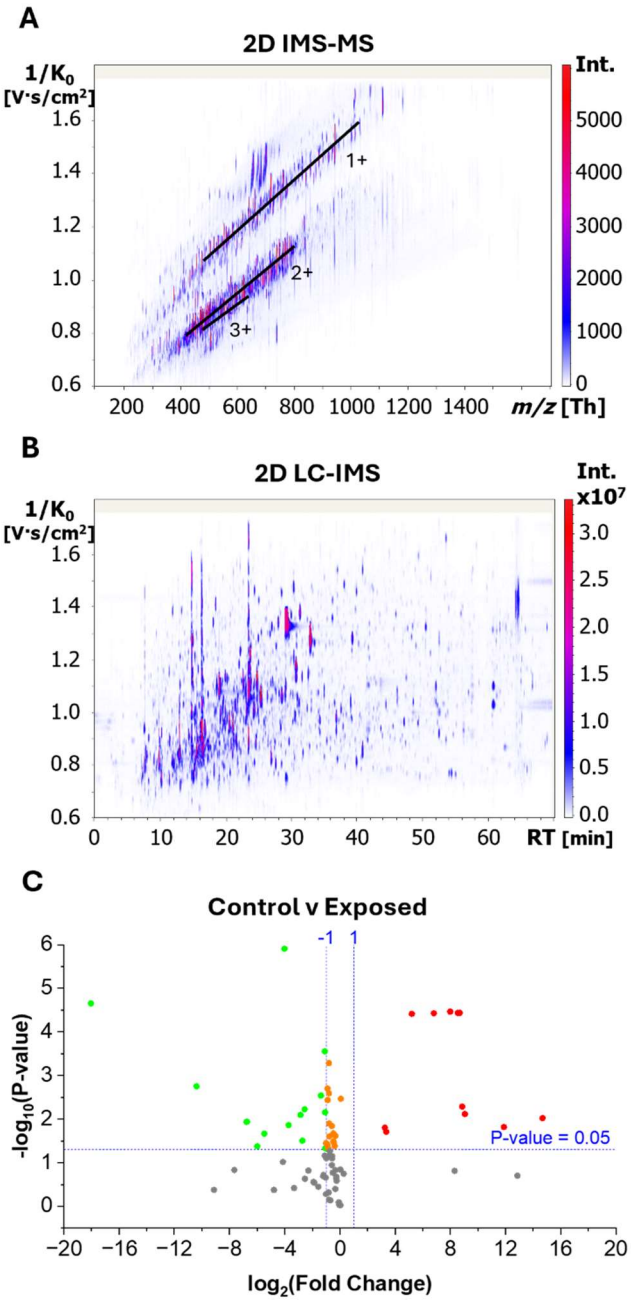

Figure 1. 2D (A) IMS-MS and (B) LC-IMS from nLC-TIMS-ddaPASEF-ToF MS/MS of bottom-up propionylated tryptic coral peptides and (C) volcano plot comparing histone PTM changes from Control to Exposed corals. The volcano plot was created by plotting the log2 of the fold change (x-axis, significance = x<-1 or x>1) and -log10 of the 1:1 comparison p-values determined by two-tailed t-test (y-axis, 95% confidence interval) using the QC1 normalized areas.

Figure 2

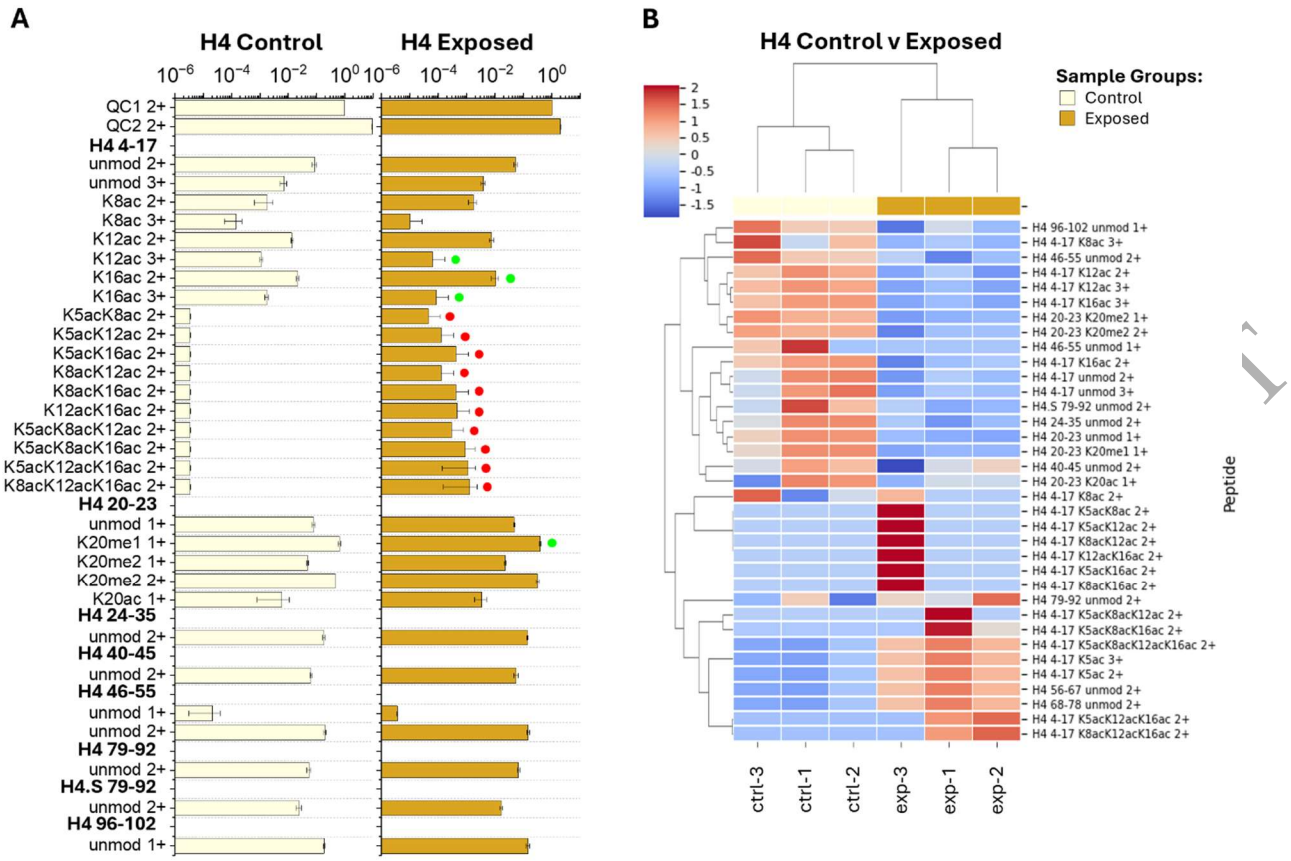

Figure 2. (A) Detected H4 bottom-up peptide areas normalized to QC1 from Control and Exposed coral samples with up- and downregulated peptide features distinguished by red and green dots, respectively. Bottom-up peptide feature bar plots shown were created from the QC1-normalized area means (bar) and standard deviations (error) across biological replicates. (B) Heatmap grouping samples (x-axis) by Control (light yellow) and Exposed (gold) corals and H4 peptides (y-axis) by *z*-score (complete comparison) of the QC1 normalized area values with dendrograms displayed using Euclidean distance.

449 **Figure 3**

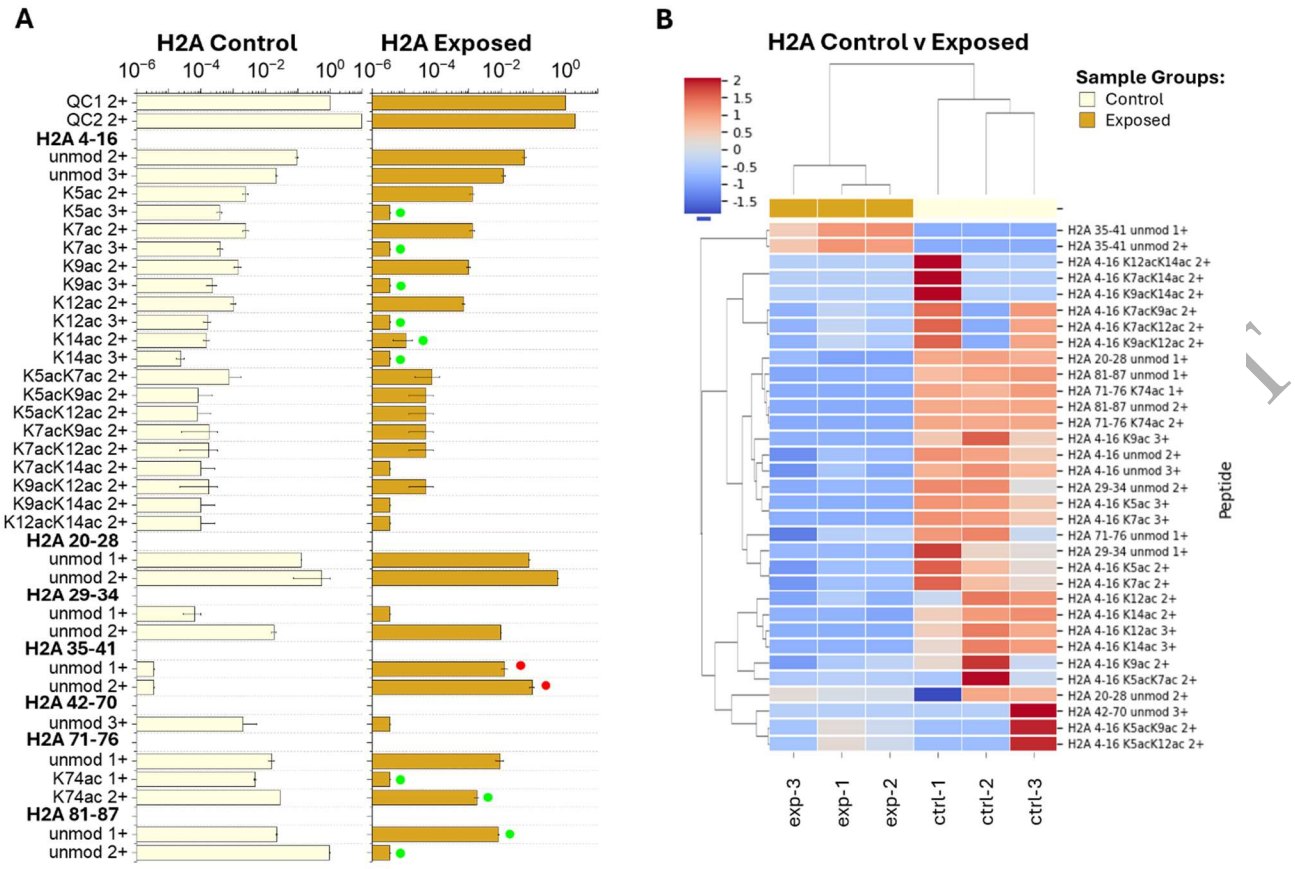

450

451 **Figure 3.** (A) Detected H2A bottom-up peptide areas normalized to QC1 from Control and Exposed coral samples
452 with up- and downregulated peptide features distinguished by red and green dots, respectively. Bottom-up peptide
453 feature bar plots shown were created from the QC1-normalized area means (bar) and standard deviations (error) across
454 biological replicates. (B) Heatmap grouping samples (x-axis) by Control (light yellow) and Exposed (gold) corals and
455 H2A peptides (y-axis) by *z*-score (complete comparison) of the QC1 normalized area values with dendrograms
456 displayed using Euclidean distance.

457

458

459 **Figure 4**

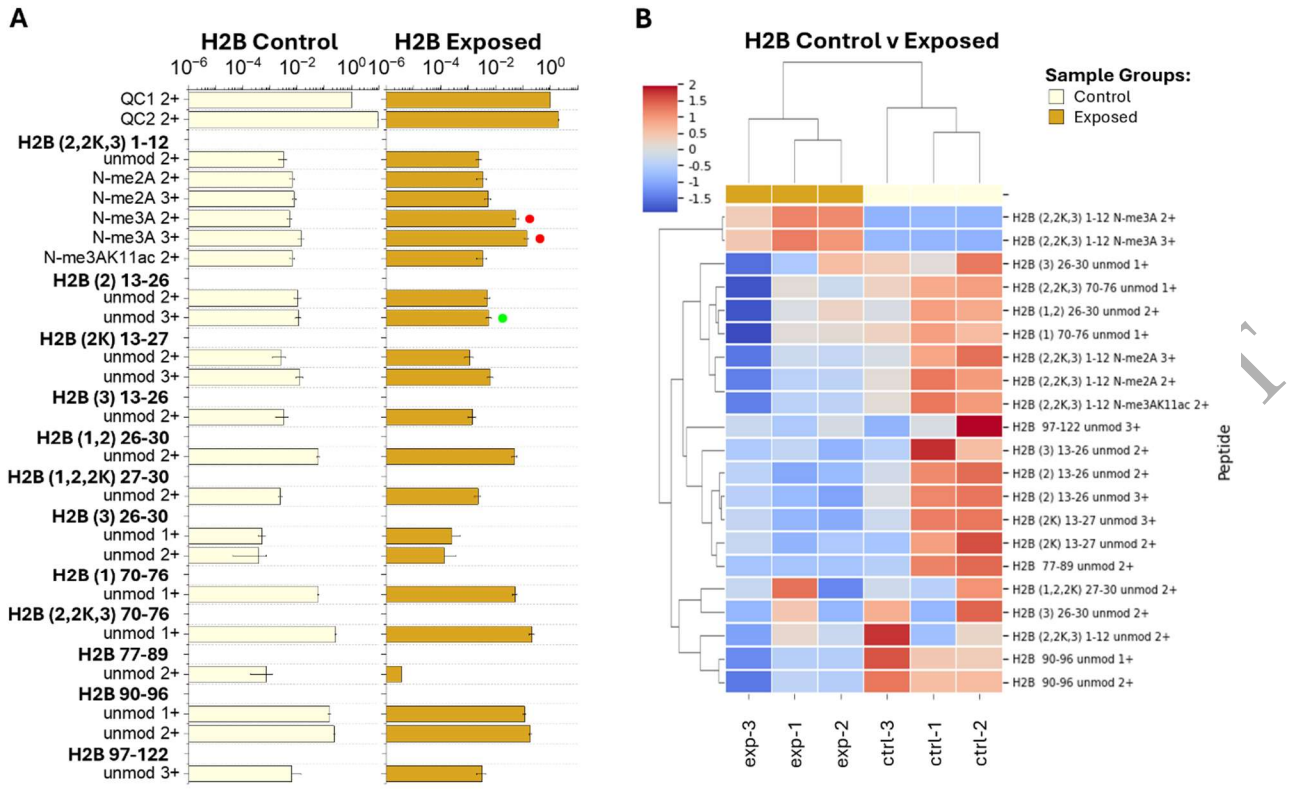

460

461 **Figure 4.** (A) Detected H2B bottom-up peptide areas normalized to QC1 from Control and Exposed coral samples
462 with up- and downregulated peptide features distinguished by red and green dots, respectively. Bottom-up peptide
463 feature bar plots shown were created from the QC1-normalized area means (bar) and standard deviations (error) across
464 biological replicates. (B) Heatmap grouping samples (x-axis) by Control (light yellow) and Exposed (gold) corals and
465 H2B peptides (y-axis) by *z*-score (complete comparison) of the QC1 normalized area values with dendrograms
466 displayed using Euclidean distance.

467